IEEE Access
Multidisciplinary ⋮ Rapid Review ⋮ Open Access Journal

Received June 4, 2019, accepted July 3, 2019, date of publication July 11, 2019, date of current version August 1, 2019.

Digital Object Identifier 10.1109/ACCESS.2019.2928225

InSb-Enhanced Thermally Tunable Terahertz Silicon Metasurfaces

DAQUAN YANG[1], CHAO ZHANG[1], XIAOGANG LI[1], AND CHUWEN LAN[1, 2]

[1]State Key Laboratory of Information Photonics and Optical Communications, School of Information and Communication Engineering, Beijing University of Posts and Telecommunications, Beijing 100876, China

[2]State Key Laboratory of Millimeter Waves, Southeast University, Nanjing 210096, China

Corresponding author: Daquan Yang (ydq@bupt.edu.cn) and Chuwen Lan (lanchuwen@bupt.edu.cn)

This research was supported in part by the Fundamental Research Funds for the Central Universities (2018XKJC05); Fund of Graduate Education Teaching Reform (2019Y006); The Opening Foundation of State Key Laboratory of Millimeter Waves (K202008); Fund of the State Key Laboratory of Information Photonics and Optical Communications (BUPT: IPOC2017ZT05), China.

ABSTRACT Terahertz silicon-based all-dielectric metasurfaces have attracted enormous attention for their promising applications. In practice, however, their tuning ability has been limited by the stability of silicon. Herein, we propose a new way to realize thermally tunable silicon metasurfaces in the terahertz region based on InSb film. To verify the feasibility of this method, a tunable all-dielectric metasurface absorber based on hybrid dielectric waveguide resonance is designed and demonstrated. The absorber consists of sub-wavelength silicon cylinders on the polydimethylsiloxane (PDMS) substrate, and an ultra-thin InSb film is deposited on it to achieve tunability. Meanwhile, by employing the other free-standing grating structure, the universality of this method is demonstrated. Notably, when the temperature increases from 300 to 400 K, the resonance shift in the grating structure can reach 0.091 THz, and good amplitude stability in the transmission spectrum is achieved. With advantages like fine tunability and easy fabrication, these all-dielectric metasurfaces may have great potential in THz high efficiency devices.

INDEX TERMS Terahertz, metamaterials, optical devices, semiconductor films, temperature dependence, thermal, tunable circuits and devices.

I. INTRODUCTION

Terahertz (THz) waves have attracted significant interest because of their potential applications in sensing, imaging, and biomedical optics [1]–[3]. However, the rapid development of THz sciences has been hampered owing to insufficient suitable materials and devices. Fortunately, metasurfaces provide a promising way to solve this problem. As the two-dimensional equivalent of metamaterials, metasurfaces respond to the incident radiation mainly through their geometrical patterns. This means that the phase, dispersion, amplitude, and polarization of THz waves can be fully controlled via freely changing metasurface design [4]–[7]. As is generally known, the scattering of electromagnetic waves on sub-wavelength cylinders bring with the excitation of electric and magnetic Mie resonances, which can substantially alter the intensity and pattern of scattering [8]. Therefore, by triggering strong localized electrical and magnetic Mie-type resonances [9]–[11], all-dielectric silicon metasurfaces (ADSM) have received special attention. Today, they are widely used in perfect absorbers, Fano resonances, magnetic mirrors, and broadband reflectors [12]–[16].

The electromagnetic responses of ADSM are difficult to change once their geometrical parameters are determined, which has caused limitations in their practical applications [17]. Therefore, further exploitation of ADSM with the ability to dynamically manipulate the incident wave is of vital importance. In recent years, various tuning mechanisms and approaches ranging from mechanical stretching to electromagnetic control have been studied and reported. Integrating with functional materials, including transparent conductive oxides, ferroelectrics, graphenes, phase change materials, liquid crystals, and semiconductors, is the most common method to realize a tunable electromagnetic response exhibited by metasurfaces [18]–[23]. Several tunable ADSM have been proposed and demonstrated. For example, considering the influence of the liquid crystals anisotropic dielectric environment on electromagnetic resonances, Sautter et al. utilize the temperature-dependent change in the permittivity of a liquid crystal to demonstrate an active tunable all-dielectric metasurface [23]. Moreover, by using metamaterial patterns consisting of graphene, the tunable resonant mechanisms of

The associate editor coordinating the review of this manuscript and approving it for publication was Shah Nawaz Burokur.

graphene-SiO_2/Si structures deposited on flexible substrates have been theoretically researched by He [24].

Considering the temperature-dependent permittivity of InSb film, we propose a new method for tunable all-dielectric silicon metasurfaces. In this manner, the properties of metasurfaces can be thermally tuned with the influence of InSb film. This paper is organized as follows. Initially, we discuss temperature-dependent permittivity of InSb film. Thereafter, we present a tunable terahertz all-dielectric silicon absorber and describe its absorption mechanism. Finally, we demonstrate the universality of our tuning method by employing a free-standing grating structure.

II. SIMULATION AND DISCUSSION

As the key materials for optoelectronics, the ability of semiconductors to tune the carrier density and refractive index renders them effective in tunable metasurfaces. It is well-known that InSb is a semiconductor that is an excellent candidate as a thermal material. Considering of the small band gap, high electron-mobility, low effective mass and electron density of InSb, the permittivity of which can be easily tuned by the change in temperature. In the THz region, the permittivity of InSb can be obtained from Drude model [25].

$$\varepsilon(\omega) = \varepsilon_\infty - {\omega_p}^2/(\omega^2 + i\gamma\omega) \quad (1)$$

where ω is the resonant frequency, $\varepsilon_\infty = 15.68$ represents the high-frequency value, and the damping constant $\gamma = 0.1\pi$ THz. The plasma frequency ω_p can be calculated by the equation:

$$\omega_p = \sqrt{Ne^2/\varepsilon_0 m} \quad (2)$$

In which N is the carrier density, m is the effective mass of free carriers, and ε_0 represents the vacuum permittivity. Therefore, we can determine the plasma frequency from (2). The intrinsic carrier density of InSb is a function of temperature, which can be adequately described in the following relationship:

$$N = 5.76 \times 10^{14} T^{3/2} exp(-0.13/kT) \quad (3)$$

where k represents the Boltzmann constant and kT is in eV, whereas N is in cm^{-3}. To provide further understanding of the InSb carrier density, we plot the relationship between the intrinsic carrier density and temperature in Figure 1(a). When the temperature increases from 300 K to 400 K, the carrier density has a remarkable enhancement from 2.051×10^{16} cm^{-3} to 1.099×10^{17} cm^{-3}. This implies that the temperature has a significant influence on the electronic properties of InSb. We calculate the permittivity of InSb with the use of (1) to (3), and the results can be obtained from Figure 1(b) [25], in which the real part of the permittivity is plotted on the left axis, and the imaginary part is plotted on the right axis as a function of temperature. The real part of the permittivity gradually increases with the decrease in temperature, while the imaginary part has the opposite tendency. These results indicate that the InSb permittivity is sensitive to the change of temperature, and we can control the properties of InSb through thermal stimulation.

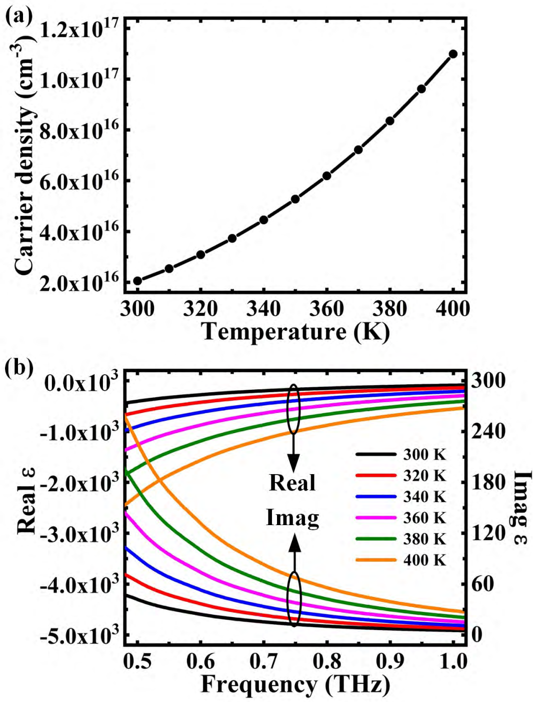

FIGURE 1. (a) The functional relationship between the carrier density of InSb and temperature. (b) Real and imaginary part of InSb permittivity at different temperatures [25].

Considering the functional relationship between permittivity and temperature, we propose to utilize InSb thin film to realize the thermal tunability of ADSM. First, we design an absorber consisting of sub-wavelength silicon cylinders on an ultra-thin polydimethylsiloxane (PDMS) substrate to verify the feasibility of this method. Then, we demonstrate the universality of its tunability performance by employing a free-standing silicon grating structure. In this study, model building and simulations are performed out using software package CST Microwave Studio.

A. ALL-DIELECTRIC METASURFACE ABSORBER

The chosen basic unit cell of the absorber is a silicon cylinder, because it can achieve spectral overlap of the magnetic and electric dipole mode through geometry tuning [26]. The schematic configuration diagram of the proposed thermally tunable ADSM THz absorber is shown in Figure 2(a). Silicon cylinders are bonded to the PDMS substrate while covered with a layer of InSb thin film, and the inset depicts the geometric view for the unit cell structure. A normal incident THz plane electromagnetic wave is assumed in the simulation, which propagates from the $z-$ direction to the $x - y$ plane. The permittivity and loss tangent of PDMS substrate can be set as 1.72 and 0.15, respectively. Silicon is chosen as the waveguide material because it realizes a permittivity of 11.0 with a relatively small loss tangent of approximately 0.06 [12], [27]. It is well known that a high absorbance is achieved when the impedance matching of free

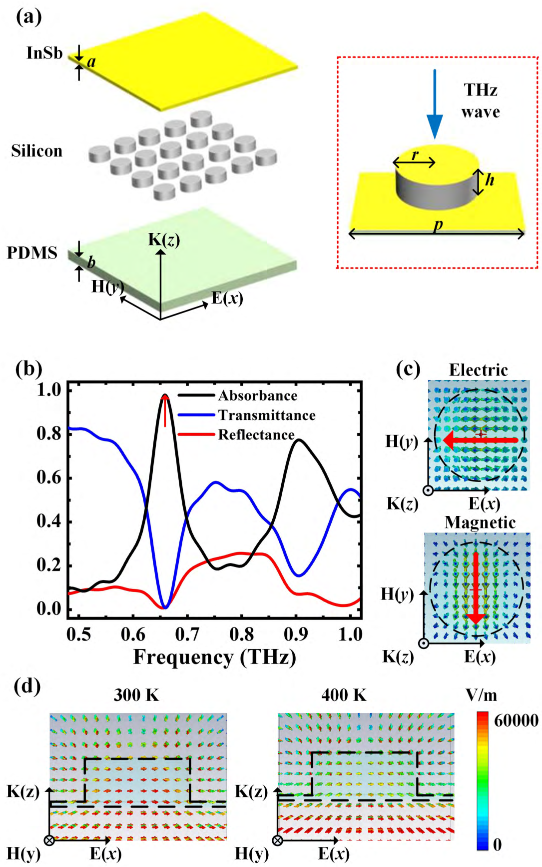

FIGURE 2. (a) The decomposition diagram of the ADSM absorber. The thickness of InSb thin film, *a*: 110 nm; the thickness of ultra-thin PDMS substrate, *b*: 8 μm. The inset is the basic unit cell dimension of the cylinder resonator, in which lattice periodicity, *p*: 210 μm; radius, *r*: 64 μm; height, *h*: 60 μm. (b) The simulated spectra of absorbance (red curve), transmittance (blue curve), and reflectance (black curve). (c) Fields of the electric and magnetic dipole modes in the $x-y$ plane within a single unit cell for a frequency of approximately 0.66 THz. The red arrow marks the direction of the electric and magnetic fields. (d) The side views of the electric field distribution in the ADSM absorber with temperatures of 300 K and 400 K, respectively. The cross section of the ADSM absorber is marked with a black dotted line.

space and a large extinction coefficient are fulfilled [12]. Therefore, hybrid dielectric waveguide resonances are utilized as the explanation of the absorbance mechanism of the designed structure [4]. Here, the all-dielectric silicon cylinders are described as waveguides when the THz wave is incident, as shown in Figure 2(a). Meanwhile, the cylindrical dielectric waveguide can support HE and EH modes at the same time. When $H_z/E_z \ll 1$, the waveguide supports the HE mode, which is transverse magnetic (TM) like as E_z is dominant. On the contrary, when $E_z \ll H_z$ and H_z is dominant, the transverse electric (TE) like EH mode appears. Three indices are denoted to describe the variation of the field within the silicon waveguide, i.e., HE_{nml} and EH_{nml}. For the proposed absorber, only the lowest order magnetic dipole (HE_{111}) and electric dipole (EH_{111}) inside the waveguide are taken into account to achieve a highly absorbing state. When resonances of EH_{111} and HE_{111} modes overlap at the same frequency, the THz wave is totally absorbed with the satisfaction of impedance matching. However, unlike the HE mode, which exists for any frequency for a given size, the EH mode has a cutoff condition. Thus, we need to find the minimum height (h) and radius (r) of the silicon cylinder that can support hybrid HE_{111} and EH_{111} modes at the same target frequency. The EH_{111} cutoff condition is given by [12]

$$r = 0.61\lambda_0/(n^2 - 1)^{1/2} \tag{4}$$

$$h = \lambda_0/2n \tag{5}$$

Utilizing (4) and (5) and considering the influence of the PDMS substrate, the parameters of the silicon cylinder are set in Figure 2(a). As we can see from the magnetic and electric field distributions in a silicon cylinder at the same frequency from Figure 2(c), the electric dipole is oriented along the $x-$axis, while the magnetic dipole is oriented along the $y-$axis simultaneously. This means that significant absorbance in the structure occurs when the magnetic dipole resonance coincides with the electric dipole resonance. Figure 2(b) presents a strong simulation absorbance peak (calculated from the corresponding transmittance and reflectance, $A(\omega) = 1-T(\omega)-R(\omega)$) for the all-dielectric silicon absorber at 0.66 THz, and the absorbance amplitude can reach above 98%. That is, the THz wave is totally absorbed due to the interaction between the electric and magnetic dipole resonances. Meanwhile, the side views of the electric field distribution in the ADSM absorber with temperatures of 300 K and 400 K are plotted in Figure 2(d). It is obviously that the electric field distribution at the resonant frequency is dependent on the environment temperature. This phenomenon is agreement with our surmise that the absorbance characteristics of the structure can be tuned through thermal.

To examine the thermal tunability of the proposed absorber structure, we simulate its absorbance spectra at different temperatures. When the temperature increases from 300 K to 400 K, the carrier density of the InSb thin film, as an augmented function of temperature, increases and changes the dielectric environment of the silicon cylinders. As indicated in Figure 3(a), the frequency of electromagnetic resonance increases from 0.659 THz to 0.683 THz when the temperature increases from 300 K to 400 K. Therefore, when the geometric parameters of the device are fixed, the absorbance frequency can be actively controlled by changing the structure temperature. Meanwhile, the absorbance amplitude at the resonant frequency decreases from 98.07% to 90.72%, which can be obtained from Figure 3(b). The above analysis shows that the overlap resonances are broken with the permittivity change in the InSb film, causing a drop in the absorbance amplitude. Meanwhile, owing to the absorbance amplitude remaining above 90%, our design can still absorb most of the incident THz wave in a wide temperature range.

Both the temperature and thickness of InSb film can influence the absorbance performance of the structure. Figure 4(a) presents the results of the simulated absorbance spectra with different thicknesses of InSb thin film when the temperature

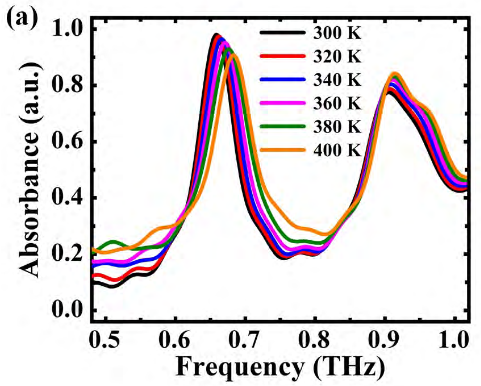

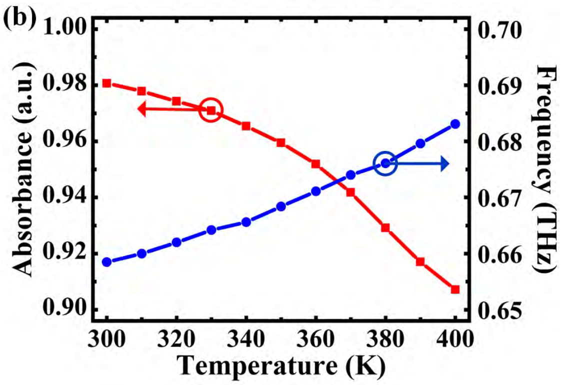

FIGURE 3. (a) The simulated absorbance spectra of the all-dielectric silicon absorber covered 110-nm-thick InSb film with temperatures of 300 K, 320 K, 340 K, 360 K, 380 K, 400 K, respectively. (b) The amplitude of the absorbance peak (red curve) is plotted on the left axis, while the absorbance frequency (blue curve) is plotted on the right axis as a function of temperature.

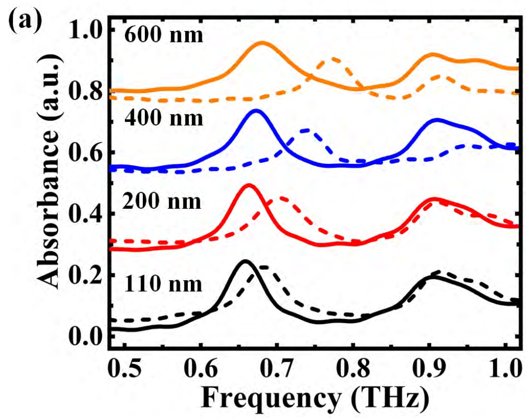

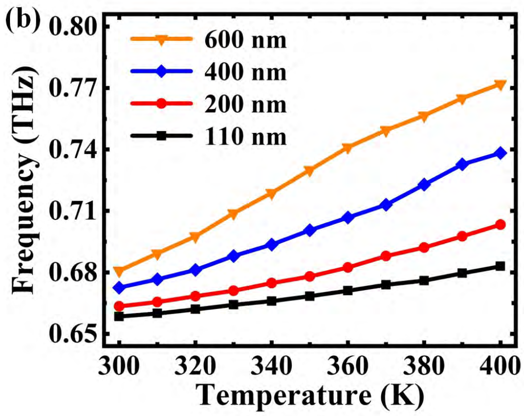

FIGURE 4. (a) Simulated absorbance spectra of the structure at 300 K (solid line) and 400 K (dotted line) with different thicknesses of the InSb thin film. The absorbance peak corresponds to the overlap of electric and magnetic dipole resonances. (b) Numerical demonstration of the absorbance frequency at various temperatures by changing the thickness of the InSb thin film.

is set to 300 K and 400 K. These results demonstrate that the resonances move to higher frequencies with increasing thicknesses when the temperature is fixed. More importantly, when the temperature arises from 300 K to 400 K, the resonance represents a wider frequency shift with increasing InSb thin film thickness, as evident from Figure 4(b). Therefore, we can conclude that the existence of InSb thin film can enhance the thermal tunability of the ADSM in the THz region, and the performance of the absorber can be further optimized.

B. ALL-DIELECTRIC SILICON GRATING

Through analysis and simulation, we have demonstrated that InSb thin film can be realized as a tunable all-dielectric silicon absorber. Herein, the free-standing silicon grating is also utilized to demonstrate that our method can be applied universally in different metasurface structures. The schematic diagram of the thermally tunable THz all-dielectric grating structure is shown in Figure 5(a). It consists of two dielectric layers in which the posterior is silicon grating and the former is InSb thin film. In the simulation, the width, w, and thickness, t, of the silicon cylinder are both 100 μm, and the period, T, is defined as 200 μm. The designed grating structure is irradiated by a normally incident TE-polarized THz wave along the $z-$axis, while the electric field is parallel to the $x-$axis, and the magnetic field is parallel to the $y-$axis based on the finite difference-time domain. The transmission spectrum and the corresponding distributions of the electric field at the resonant frequencies are simulated and provided in Figure 5(b), where two distinct resonance dips can be observed at 0.631 THz and 0.852 THz, respectively. The first resonance mode (M1) can be confirmed as a magnetic dipole resonance through the electric field, in which we can observe a clear current loop. The second resonance mode (M2) can be defined as a magnetic quadrupole resonance, homologous to the two current loops that appear in another electric field distribution. The side views of the grating electric field distribution at the second resonant mode are also simulated and provided in Figure 5(c). When temperature increases from 300 K to 400 K, a stronger electric field distribution can be observed inside the grating. Since the permittivity of grating is a consistent, we can speculate that this change is caused by the InSb film with temperature-dependent permittivity, as discussed in detail below.

To confirm the thermal tunability of the grating structure, the temperature dependence of transmission is studied by increasing the temperature from 300 K to 400 K, as the corresponding spectra are plotted in Figure 6(a).

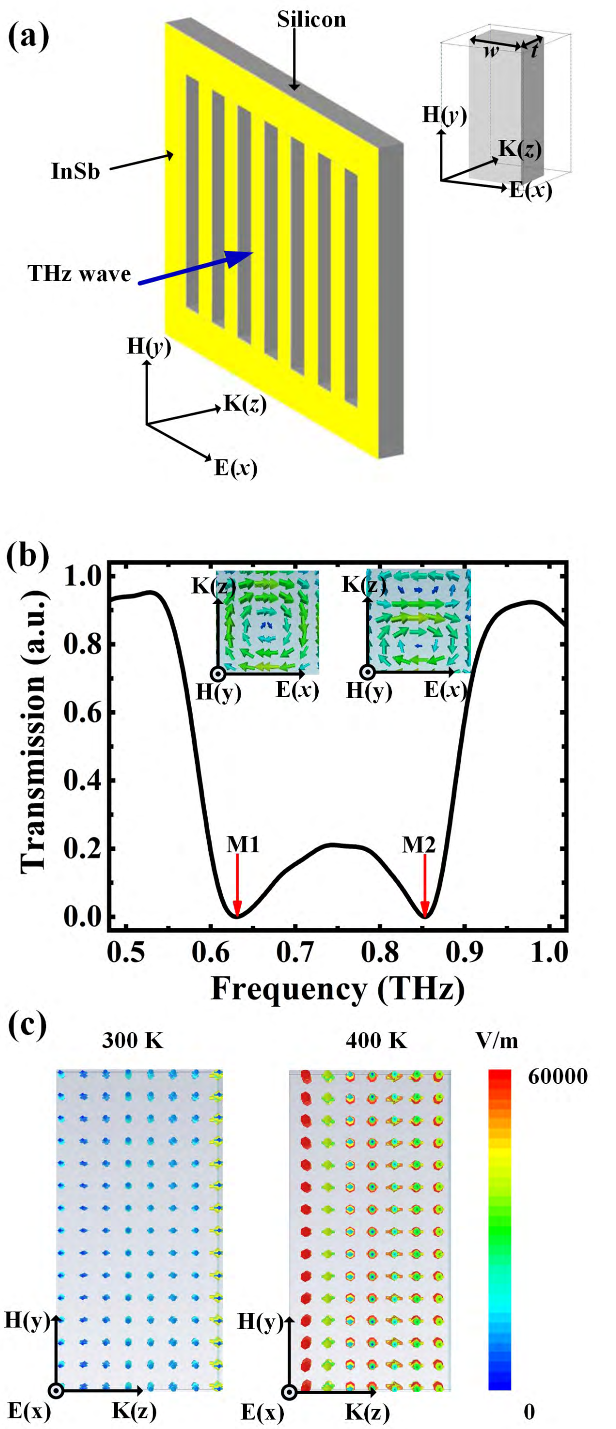

FIGURE 5. (a) Schematic illustration of the one-dimensional silicon grating covered with InSb thin film, the inset is a unit cell structure without InSb thin film. (b) Simulated transmission spectrum for TE polarization of the proposed structure at 300 K. The insets are the electric field distributions of the resonances. The red arrows mark the position of resonance modes in silicon grating. (c) The side views of the electric field distribution of the second resonance mode with temperatures of 300 K and 400 K, respectively.

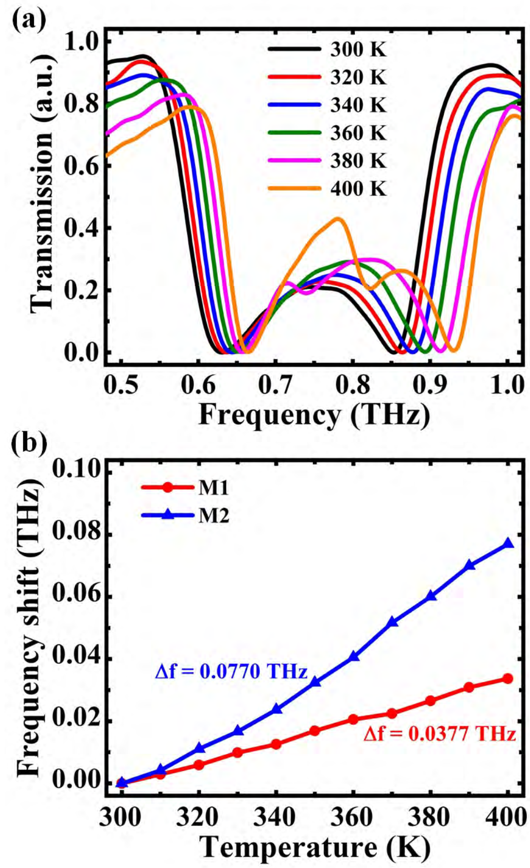

FIGURE 6. (a) The corresponding simulated transmission spectra of the metasurface composed by silicon grating and a layer of InSb thin film. (b) The frequency shift of resonances are given as a function of temperature.

The frequencies of the resonances both have a blue shift with the increase in temperature. A more detailed analysis is further clarified in Figure 6(b), in which a temperature increase from 300 K to 400 K corresponds to a blue-shift in the fundamental resonance mode (red curve) of 0.033 THz (from 0.631 THz to 0.664 THz), while the second-order resonance mode (blue curve) experiences a greater blue-shift of 0.077 THz (from 0.853 THZ to 0.930 THz). In our previous work, an active tunable silicon-based all-dielectric metasurface integrated with VO_2 film was designed, fabricated, and demonstrated [28]. Although the two structures achieve a comparable tuning range, the transmission amplitude of the grating structure, based on the InSb film proposed here, is almost unchanged. This result suggests the amplitude stability of this method in the tuning process, which is indispensable in practical application.

Clearly, the thermal tunability of the grating structure is also dependent on the thickness of the InSb thin film, which we can speculate from the enhanced frequency shift in the absorber structure in Figure 4. To verify this speculation, the calculation results are presented in Figure 7, with the thicknesses of the InSb thin film set to 200 nm, 400 nm, and 600 nm. As evident from Figure 7(b), the range of the second-order mode resonance frequency offsets from 0.035 THz to 0.082 THz when the thickness increases from 200 nm to 600 nm. This is similar to the increase in the

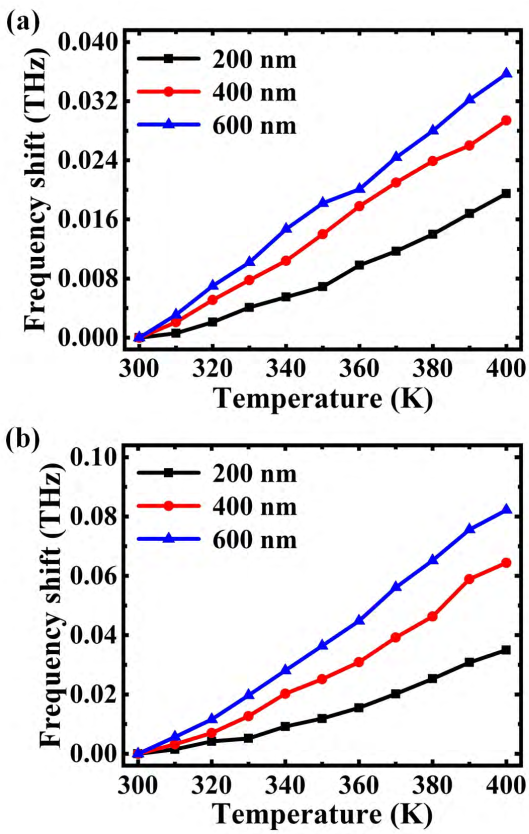

FIGURE 7. The resonance frequency shift of (a) the fundamental mode and (b) the second-order mode with different InSb thin film thickness.

resonance frequency range of the absorber from 0.039 THz to 0.091 THz for the same situation in Figure 4(b). This means that our approach is applicable to different metasurface structures. Therefore, we can conclude that this new proposed method to realize thermally tunable silicon metasurfaces based on InSb film is practical in the terahertz region.

III. CONCLUSION

We have proposed a new way to realize thermally tunable ADSM in the terahertz region based on InSb film. In this new method, an ultra-thin InSb film is deposited on the all-dielectric silicon metasurfaces to achieve tunability. The simulations of the absorber and grating reveal that the Mie type resonances in unit cell can be enhanced with the existence of InSb thin film, which possesses a temperature-dependent permittivity. This new method provides a practical approach to realize the tunability of all-dielectric metasurfaces and can further inspire various THz metasurface applications.

REFERENCES

[1] C. Russell, M. Swithenbank, C. D. Wood, A. D. Burnett, L. Li, E. H. Linfield, A. G. Davies, and J. E. Cunningham, "Integrated on-chip THz sensors for fluidic systems fabricated using flexible polyimide films," *IEEE Trans. THz Sci. Technol.*, vol. 6, no. 4, pp. 619–624, Jul. 2016.

[2] M. Tonouchi, "Cutting-edge terahertz technology," *Nature Photon.*, vol. 1, no. 2, pp. 97–105, 2007.

[3] X. Yang, X. Zhao, K. Yang, Y. Liu, Y. Liu, W. Fu, and Y. Luo, "Biomedical applications of terahertz spectroscopy and imaging," *Trends Biotechnol.*, vol. 34, no. 10, pp. 810–824, Oct. 2016.

[4] S. H. Zhou, Z. Shen, R. Kang, S. Ge, and W. Hu, "Liquid crystal tunable dielectric metamaterial absorber in the terahertz range," *Appl. Sci.*, vol. 8, no. 11, pp. 2211–2217, Nov. 2018.

[5] A. Arbabi, Y. Horie, M. Bagheri, and A. Faraon, "Dielectric metasurfaces for complete control of phase and polarization with subwavelength spatial resolution and high transmission," *Nature Nanotechnol.*, vol. 10, no. 11, pp. 937–943, 2015.

[6] Y. Yang, W. Wang, P. Moitra, I. I. Kravchenko, D. P. Briggs, and J. Valentine, "Dielectric meta-reflectarray for broadband linear polarization conversion and optical vortex generation," *Nano Lett.*, vol. 14, no. 3, pp. 1394–1399, Feb. 2014.

[7] M. Decker, I. Staude, M. Falkner, J. Dominguez, D. N. Neshev, I. Brener, T. Pertsch, and Y. S. Kivshar, "High-efficiency dielectric Huygens' surfaces," *Adv. Opt. Mater.*, vol. 3, no. 6, pp. 813–820, 2015.

[8] S. Kruk and Y. Kivshar, "Functional meta-optics and nanophotonics governed by Mie resonances," *ACS Photon.*, vol. 4, no. 11, pp. 2638–2649, Oct. 2017.

[9] X. Liu, C. Lan, K. Bi, B. Li, Q. Zhao, and J. Zhou, "Dual band metamaterial perfect absorber based on Mie resonances," *Appl. Phys. Lett.*, vol. 109, no. 6, pp. 62902–62906, Aug. 2016.

[10] Q. Wang, F. Zhang, Y. Xiong, Y. Wang, X.-Z. Tang, C. Jiang, I. Abrahams, and X. Huang, "Dual-band binary metamaterial absorber based on low-permittivity all-dielectric resonance surface," *J. Electron. Mater.*, vol. 48, no. 2, pp. 787–793, Feb. 2019.

[11] K. E. Chong, I. Staude, A. James, J. Dominguez, S. Liu, S. Campione, G. S. Subramania, T. S. Luk, M. Decker, D. N. Neshev, I. Brener, and Y. S. Kivshar, "Polarization-independent silicon metadevices for efficient optical wavefront control," *Nano Lett.*, vol. 15, no. 8, pp. 5369–5374, 2015.

[12] K. Fan, J. Y. Suen, X. Liu, and W. J. Padilla, "All-dielectric metasurface absorbers for uncooled terahertz imaging," *Optica*, vol. 4, no. 6, pp. 601–604, May 2017.

[13] B. Hopkins, D. S. Filonov, A. E. Miroshnichenko, F. Monticone, A. Alu, and Y. S. Kivshar, "Interplay of magnetic responses in all-dielectric oligomers to realize magnetic Fano resonances," *ACS Photon.*, vol. 2, no. 6, pp. 724–729, May 2015.

[14] Z. J. Ma, S. M. Hanham, P. Albella, B. Ng, H. T. Lu, Y. Gong, S. A. Maier, and M. Hong, "Terahertz all-dielectric magnetic mirror metasurfaces," *ACS Photon.*, vol. 3, no. 6, pp. 1010–1018, May 2016.

[15] P. Moitra, B. A. Slovick, W. Li, I. I. Kravchencko, D. P. Briggs, S. Krishnamurthy, and J. Valentine, "Large-scale all-dielectric metamaterial perfect reflectors," *ACS Photon.*, vol. 2, no. 6, pp. 692–698, May 2015.

[16] D. Q. Yang, C. Zhang, K. Bi, and C. W. Lan, "High-throughput and low-cost terahertz all-dielectric resonators made of polymer/ceramic composite particles," *IEEE Photon. J.*, vol. 11, no. 1, Feb. 2019, Art. no. 5900408.

[17] C. Luo, D. Li, J. Yao, and F. Ling, "Direct thermal tuning of the terahertz plasmonic response of semiconductor metasurface," *J. Electromagn. Waves Appl.*, vol. 29, no. 18, pp. 2512–2522, Dec. 2015.

[18] Y.-W. Huang, H. W. H. Lee, R. Sokhoyan, R. A. Pala, K. Thyagarajan, S. Han, D. P. Tsai, and H. A. Atwater, "Gate-tunable conducting oxide metasurfaces," *Nano Lett.*, vol. 16, pp. 5319–5325, Aug. 2016.

[19] B.-X. Wang, X. Zhai, G.-Z. Wang, W.-Q. Huang, and L.-L. Wang, "Frequency tunable metamaterial absorber at deep-subwavelength scale," *Opt. Mater. Express*, vol. 5, no. 2, pp. 227–235, Feb. 2015.

[20] A. C. Tasolamprou, A. D. Koulouklidis, C. Daskalaki, C. P. Mavidis, G. Kenanakis, G. Deligeorgis, Z. Viskadourakis, P. Kuzhir, S. Tzorzakis, M. Kafesaki, E. N. Economou, and C. M. Soukoulis, "Experimental demonstration of ultrafast THz modulation in a graphene-based thin film absorber through negative photoinduced conductivity," *ACS Photon.*, vol. 6, no. 3, pp. 720–729, Feb. 2019.

[21] H. Cai, S. Chen, C. Zou, Q. Huang, Y. Liu, X. Hu, Z. Fu, Y. Zhao, H. He, and Y. Lu, "Multifunctional hybrid metasurfaces for dynamic tuning of terahertz waves," *Adv. Opt. Mater.*, vol. 6, no. 14, Jul. 2018, Art. no. 1800257.

[22] Z.-X. Shen, S.-H. Zhou, S.-J. Ge, W. Hu, and Y.-Q. Lu, "Liquid crystal enabled dynamic cloaking of terahertz Fano resonators," *Appl. Phys. Lett.*, vol. 114, Jan. 2019, Art. no. 041106.

[23] J. Sautter, I. Staude, M. Decker, E. Rusak, D. N. Neshev, I. Brener, and Y. S. Kivshar, "Active tuning of all-dielectric metasurfaces," *ACS Nano*, vol. 9, no. 4, pp. 4308–4315, 2015.

[24] X. He, "Tunable terahertz graphene metamaterials," *Carbon*, vol. 82, pp. 229–237, Feb. 2015.

[25] J. Zhu, J. Han, Z. Tian, J. Gu, Z. Chen, and W. Zhang, "Thermal broadband tunable terahertz metamaterials," *Opt. Commun.*, vol. 284, no. 12, pp. 3129–3133, 2011.

[26] A. E. Miroshnichenko, A. B. Evlyukhin, Y. F. Yu, R. M. Bakker, A. Chipouline, A. I. Kuznetsov, B. Luk'yanchuk, B. N. Chichkov, and Y. S. Kivshar, "Nonradiating anapole modes in dielectric nanoparticles," *Nat Commun.*, vol. 6, no. 1, Aug. 2015.

[27] X. Liu, I. V. Shadrivov, K. Fan, and W. J. Padilla, "Experimental realization of a terahertz all-dielectric metasurface absorber," *Opt. Express*, vol. 25, no. 1, pp. 191–201, Jan. 2017.

[28] C. Lan, H. Ma, M. Wang, Z. Gao, K. Liu, K. Bi, J. Zhou, and X. Xin, "Highly efficient active all-dielectric metasurfaces based on hybrid structures integrated with phase-change materials: From terahertz to optical ranges," *ACS Appl. Marer. Inter.*, vol. 11, no. 15, pp. 14229–14238, Mar. 2019.

DAQUAN YANG was born in Shandong, China, in 1986. He received the B.S. degrees in electronic information science and technology from the University of Jinan, China, in 2005, the Ph.D. degree in information and communication engineering from the Beijing University of Posts and Telecommunications (BUPT), China, in 2014. He was a Visiting Follow with Harvard University, from 2012 to 2014. He is currently an Associate Professor of BUPT. His research interests include micro/nano optics sensing and THz devices.

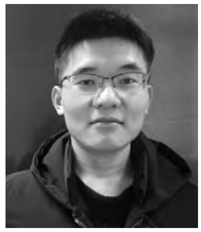

CHAO ZHANG was born in Jiangsu, China, in 1995. He received the B.S. degree in communication engineering from Nantong University, Jiangsu, China, in 2018. He is currently pursuing the M.S. degree in information and communication engineering with the Beijing University of Posts and Telecommunications. His current research interest includes THz devices.

XIAOGANG LI was born in Hubei, China, in 1996. He received the B.S. degree in communications engineering from CAUC, Tianjin, China, in 2018. He is currently pursuing the M.S. degree in information and communication engineering with Beijing University of Posts and Telecommunications. His current research interest includes micro/nano optics devices design.

CHUWEN LAN was born in Jiangxi, China, in 1990. He received the B.S. degree in optical information science and technology from the Minzu University of China, Beijing, China, in 2012, and the Ph.D. degree from the Tsinghua University of China, Beijing, in 2017. He is currently a Postdoctoral Fellow with the State Key Laboratory of Information Photonics and Optical Communications, School of Information and Communication Engineering, Beijing University of Posts and Telecommunications. His research interests include metamaterials, THz technology, and optical communications.